SUPPLEMENTAL MATERIAL

Molecular characterisation of Lupus Low Disease Activity State (LLDAS) and DORIS remission by whole-blood transcriptome-based pathways in a pan-European systemic lupus erythematosus cohort

Table of Contents

Parodis I, *et al. Ann Rheum Dis* 2024; 83:889–900. doi: 10.1136/ard-2023-224795

RNA sequencing

Total RNA was extracted from whole-blood (WB) samples collected in Tempus tubes using Tempus Spin technology (Applied Biosystems). Samples were processed in 5 batches, randomised to four 96-well plates with respect to diagnosis, recruitment center, and RNA extraction date. The samples were depleted of alpha- and beta-globin mRNAs using globinCLEAR protocol (Ambion) and 1 µg of total RNA as input. Subsequently, 400 ng of globin-depleted total RNA was used for library synthesis with TruSeq Stranded mRNA HT kit (Illumina). The libraries were quantified using qPCR with PerfeCTa NGS kit (Quanta Biosciences), and equimolar amounts of samples from the same 96-well plate were pooled. Four pools were clustered on a high output flow cell (two lanes per pool) using HiSeq SR Cluster kit v4 and the cBot instrument (Illumina). Subsequently, 50 cycles of single-read sequencing were performed on a HiSeq2500 instrument using a HiSeq SBS kit v4 (Illumina). The clustering and sequencing steps were repeated for a total of three runs in order to generate sufficient number of reads per sample. The raw sequencing data for each run were preprocessed using bcl2fastq software and the quality was assessed using FastQC tools.[1] Cutadapt[2] was used to remove 3' end nucleotides below 20 Phred quality score and extraneous adapters; additionally, reads below 25 nucleotides after trimming were discarded. Reads were then processed and aligned to the UCSC Homo sapiens reference genome (Build hg19) using STAR v2.5.2b.[3] A 2-pass mapping with default alignment parameters was used. To produce the quantification data, we used RSEM v1.2.31[4] resulting in gene level expression estimates (Transcripts Per Million |TPM] and read counts). A sample would pass the RNA single quality control (QC) if (i) the number of reads mapped to the genes was more than 7 million, and (ii) the RNA integrity number (RIN) value was higher than 7.

Parodis I, *et al. Ann Rheum Dis* 2024; 83:889–900. doi: 10.1136/ard-2023-224795

Gene-set functional annotation

To characterise functional annotations at the patient level, individualised functional annotation was performed by means of the Functional Analysis of Individual Microarray Expression (FAIME) algorithm[5, 6] that translates gene-level measurements of each sample into individual molecular function profiles. First, data were transformed by means of Variance Stabilising Transformation (VST)[7] via the DESeq2 package.[8] FAIME scores were then built considering Reactome[9] pathways mapped by at least 5 genes/transcripts; Entrez IDs that had no official gene symbols were dropped from the analysis. Reactome annotations were downloaded from the Reactome website.[10]

Differential expression pathway analysis

The main outcomes were Lupus Low Disease Activity State (LLDAS; reference: non-LLDAS) and Definitions of Remission in SLE (DORIS) remission (reference: non-remission). We also employed forward difference coding to compare LLDAS exclusive of remission with (i) non-LLDAS and (ii) DORIS remission. Importantly, the first comparison i.e., between patients fulfilling the DORIS remission criteria and patients fulfilling the criteria for LLDAS upon exclusion of those fulfilling the criteria for DORIS remission, given the fact that the two populations are independent, is the method of choice for testing the hypothesis of no difference between the overlapping samples of patients in LLDAS and patients in DORIS remission.[11] Differences between groups were calculated using linear models with a procedure akin to the voom method described by Law *et al.*[12], as described below.

An ordinary least square (OLS) regression model was fit to FAIME scores taking into account sequencing batch, gender, age, disease duration, and the use of hydroxychloroquine as covariates, along with the respective outcome (note that other therapies were not included as confounding factor in the models to avoid collinearity since they constitute components of the outcomes or are more prevalent in non-LLDAS/non-remission patients). OLS eigenvalues were checked and the variable in the design matrix with scores < 1.10^{-4} were iteratively removed so as that individual variance inflation factors (VIF) were all < 5, to avoid multicollinearity and inflation of coefficient estimates. Residual standard deviations for OLS with the multicollinearity-weighted design matrix were then calculated and plotted against average FAIME scores.

A locally weighted scatterplot smoothing (LOWESS) trend was fitted to the residual standard deviations. To better account for ties, trends in the upper and lower 5% percentiles were independently calculated. The pathway-wise square-root residual standard deviations plotted against average FAIME scores and the LOWESS fit is represented here below:

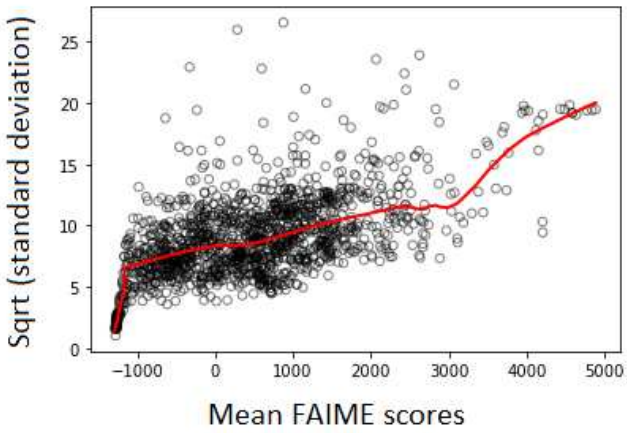

The LOWESS trend was then used to predict the standard deviation of each individual FAIME score; the inverse squared predicted standard deviation was retained as individual weight/pathway.

A weighted least square (WLS) model was fitted for each pathway using the same design matrix used to run the OLS above and the individual weights as calculated above.

Summary data from WLS models were then used to calculate a moderated t-test statistic, according to the eBayes method described by Smyth *et al.*[13], as described below.

The ordinary t-test statistic for the *p*th pathway and *k*th contrast is given by:

$$(1) \qquad t_{pk} = \frac{\beta_{pk}}{SE(\beta_{pk})} = \frac{\beta_{pk}}{s_p u_{pk}} \;\; ; \;\; s_p^2 = \frac{\mathrm{RSS}}{d_p} \;\; ; \;\; u_{pk} = \frac{SE(\beta_{pk})}{s_p}$$

where β_{pk} is the regression coefficient and $SE(\beta_{pk})$ its standard error, equivalent to the sample residual standard deviation s_p (i.e the square root of the sample residual variance s_p^2), multiplied by u_{pk} the unscaled standard deviation. In the equation, RSS is the residual sum of squares and d_p the degree of freedom of the model given by *n – k – 1.*

The moderated t-test statistic is the weighted version of the t-test that accounts for extra information borrowed from all the pathways and is given by:

$$(2) \qquad \tilde{t}_{pk} = \frac{\beta_{pk}}{\tilde{s}_p u_{pk}} \;\; ; \;\; \tilde{s}_p^2 = \frac{d_p s_p^2 + d_0 s_0^2}{d_p + d_0} \;\; ; \;\; \frac{1}{\tilde{s}_p^2} \sim \frac{1}{d_0 s_0^2} \chi_{d_0}^2$$

Where $\tilde{s}_p$ represents the posterior value of the residual variance. A scaled inverse chi-square prior is assigned to $\tilde{s}_p^2$ and the hyperparameters d_0 and s_0^2 represent the prior degrees of freedom and location of the distribution.

According to Smyth *et al.*,[13] the marginal distribution of s_p^2 follows a scaled F-distribution with degrees of freedom d_0 and d_p and is described by:

$$E(\log s_p^2) = \log s_0^2 + \psi\left({}^{d_p}/_{2}\right) - \psi\left({}^{d_0}/_{2}\right) + \log\left({}^{d_0}/_{d_p}\right) \quad (3)$$

$$var\,(log\ s_p^2) = \psi'\left({}^{d_p}/_{2}\right) + \psi'\left({}^{d_0}/_{2}\right) \quad (4)$$

Let e_p be the adjusted logarithm of sample variance of pathway p:

$$e_p = log\ s_p^2 - \psi\left({}^{d_p}/_{2}\right) + log\left({}^{d_p}/_{2}\right) \quad (5)$$

It has an expected value of:

$$E(e_p) = log\ s_0^2 - \psi\left({}^{d_0}/_{2}\right) + log\left({}^{d_p}/_{2}\right) \quad (6)$$

And variance:

$$var(e_p) = \psi'\left({}^{d_p}/_{2}\right) + \psi'\left({}^{d_0}/_{2}\right) \quad (7)$$

Thus, solving eq. (7) and applying Bassel's correction, we obtain:

$$\psi'\left({}^{d_0}/_{2}\right) = \frac{1}{p}\sum_{p=1}^{p}\frac{p}{p-1}\,(e_p - \bar{e})^2 - \psi'\left({}^{d_p}/_{2}\right) \quad (8)$$

From (8), d_0 can be found solving the inverse trigamma function.

Finally, s_0^2 can be estimated by Newton's formula:

$$s_0^2 = \exp\left\{\bar{e} + \psi\left({}^{d_0}/_{2}\right) - log\left({}^{d_0}/_{2}\right)\right\} \quad (9)$$

$s_0^2, s_p^2$and $d_0, d_p$are thus used to estimate $\tilde{s}_p^2$ and $\tilde{t}_{pk}$as described in eq. (2).

From $\tilde{t}_{pk}$ values, the corresponding moderated *p* values are computed from the t distribution with $d_0 + d_p$ degree of freedom. The *p* values are then corrected for multiple tests via the false discovery rate (FDR) method (*q*).[14]

Winsorised 20% data were used to determine a *robust moderated t-test* $\tilde{t}_{pk(r)}$ and the *robust effect size* (d_r).[15] To this end, winsorisation was independently applied to cases and controls (e.g., LLDAS/non-LLDAS, DORIS remission/non-remission), and OLS, WLS, and the eBayes procedures were run as described above.

From $\widetilde{t}_{pk(r)}$, pathway-related unscaled d_r, d^*_{rp}, were calculated according to Rosnow:[16]

$$(12) \qquad d^*_{rp} = \frac{n\,\tilde{t}_{pk(r)}}{\sqrt{d_{0(r)} + d_{p(r)}} + \sqrt{n_{out}\,\overline{n_{out}}}}$$

Where *n* is the total number of cases, n_{out} the number of subjects with the outcome of interest, and $\overline{n_{out}}$ the number of subjects without the outcome.

The d^*_{rp} found in (12) is then scaled according to Algina *et al.*[17] to produce the robust estimator d_{rp}:

$$(13) \qquad d_{rp} = .642\; d^*_{rp}$$

As an additional measure of effect size, we also calculated the *probability of superiority[18] (A)*, defined as the probability that a person picked at random from the case group will have a higher score than a person picked at random from the control group:

$$(14) \qquad A = \Phi\,\frac{d_{rp}}{\sqrt{2}}$$

where Φ is the cumulative distribution function of the standard normal distribution.

Annotations with $q<0.05$ and a $|dr|\geq 0.36$, which corresponds to a moderate effect size,[19] were considered significant.

Reactome pathways were annotated to their root terms and their different distribution in relation to a negative or positive *dr*, suggesting a downregulation or an upregulation in patients in LLDAS/ DORIS remission compared with patients who were not in LLDAS/remission, was calculated by means of the chi-squared (χ^2) test with FDR-adjusted p values; root terms with low prevalence were eliminated.

Pathway analysis with quantitative traits

For explorative purposes, associations between Reactome pathways and Systemic Lupus Erythematosus Disease Activity Index 2000 (SLEDAI-2K) scores were assessed. For each pathway, a *moderated robust t-test statistic* $\tilde{t}_{pk}$ and relative *q* values were calculated as described above from winsorised data. To determine the effect size or multivariable WLS regression, the (robust) Cohen's f^2 was calculated from *moderated robust t-test statistic* $\tilde{t}_{pk(r)}$ values calculated from winsorised data.

$$(15) \quad f^2 = \frac{r^2_{part}}{1 - r^2_{part}} \quad ; \quad r^2_{part} = \frac{\tilde{t}_{pk(r)}{}^2}{\tilde{t}_{pk(r)}{}^2 + d_{0(r)} + d_{p(r)}}$$

Where r^2_{part} is the partial coefficient of determination for the *p*th pathway and *k*th contrast.

Thresholds for f^2 interpretation are provided by Cohen[20] and are 0.02 for small, 0.15 for medium, and 0.35 for large effect size.

For all the analyses, custom codes written in python by LB built on top of the scikit-learn[21] and Statmodels[22] modules were used.

For visualisation of data, confounding factors were removed calculating residuals from WLS in a procedure akin to the removeBatchEffect function of the Limma R package;[23] clustering by means of the k-means algorithm and heatmap representation was made via the Python library Matplotlib;[24] the number of clusters was selected to obtain the highest statistical separation (e.g., chi-squared test values) of the binary outcome status across groups.

Druggability of Reactome pathways

Exploration of druggable Reactome pathways i.e., drug-target interactions was explored via the Reactome pathway browser as described in: https://idg.reactome.org/documentation/userguide#drug-target-interactions. Examples are provided to illustrate potential implications inferred from our findings.

Supplemental Figure S1. Venn diagram delineating differentially enriched pathways across different outcomes and SLEDAI-2K scores.

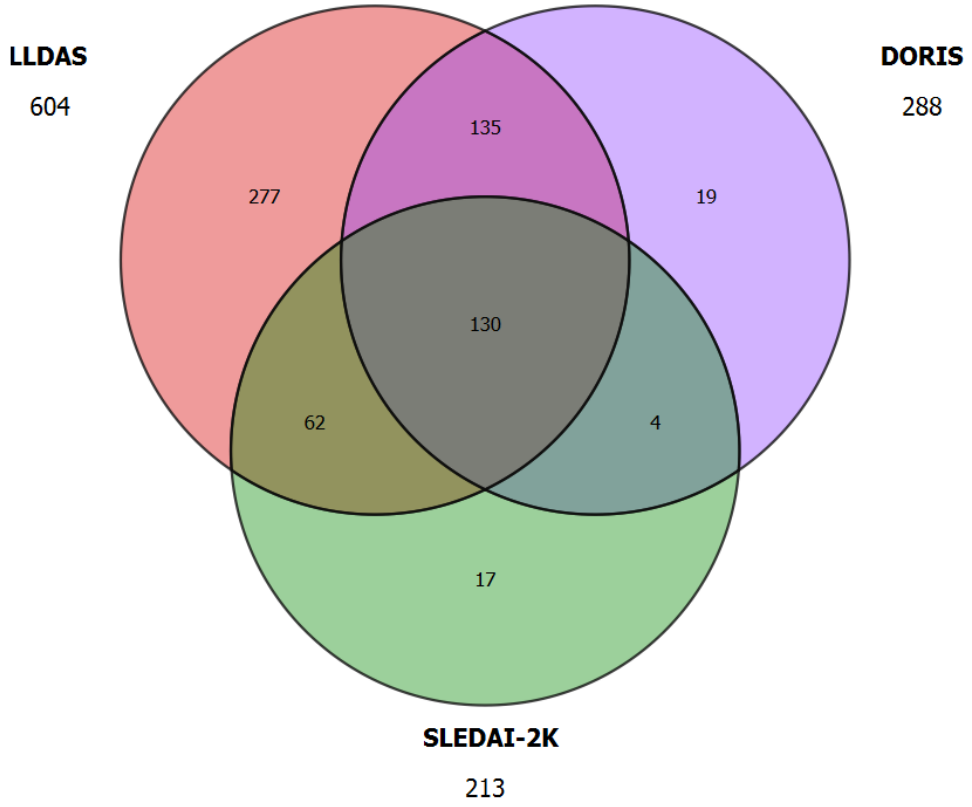

The numbers indicate differentially enriched Reactome pathways in systemic lupus erythematosus (SLE) patients with different outcomes. DORIS: Definitions of Remission in SLE; LLDAS: Lupus Low Disease Activity State; SLEDAI-2K: Systemic Lupus Erythematosus Disease Activity Index 2000.

Supplemental Figure S2. Druggable Toll-Like Receptor (TLR) cascades. Drug-pathway interactions within TLR cascades associated with definitions of remission in systemic lupus erythematosus (DORIS) remission (from: https://idg.reactome.org, with modifications); irrelevant pathways are blurred. Panel A depicts TLR 7/8, TLR9, TLR2, TLR5, and TLR10 pathways; pathway-drug interactions with TLR7 and TLR9 are highlighted with red squares (the number of related drugs is indicated) and detailed in panels B and C. The MyD88:MAL(TIRAP) cascade initiated on the plasma membrane, highlighted with red arrows and detailed in panel D, is the terminal effector of TLR2, TLR5, and TLR10 pathways. Within this pathway, Bruton Tyrosine Kinase (BTK) is a key druggable component, whose inhibitors are detailed in panel E.

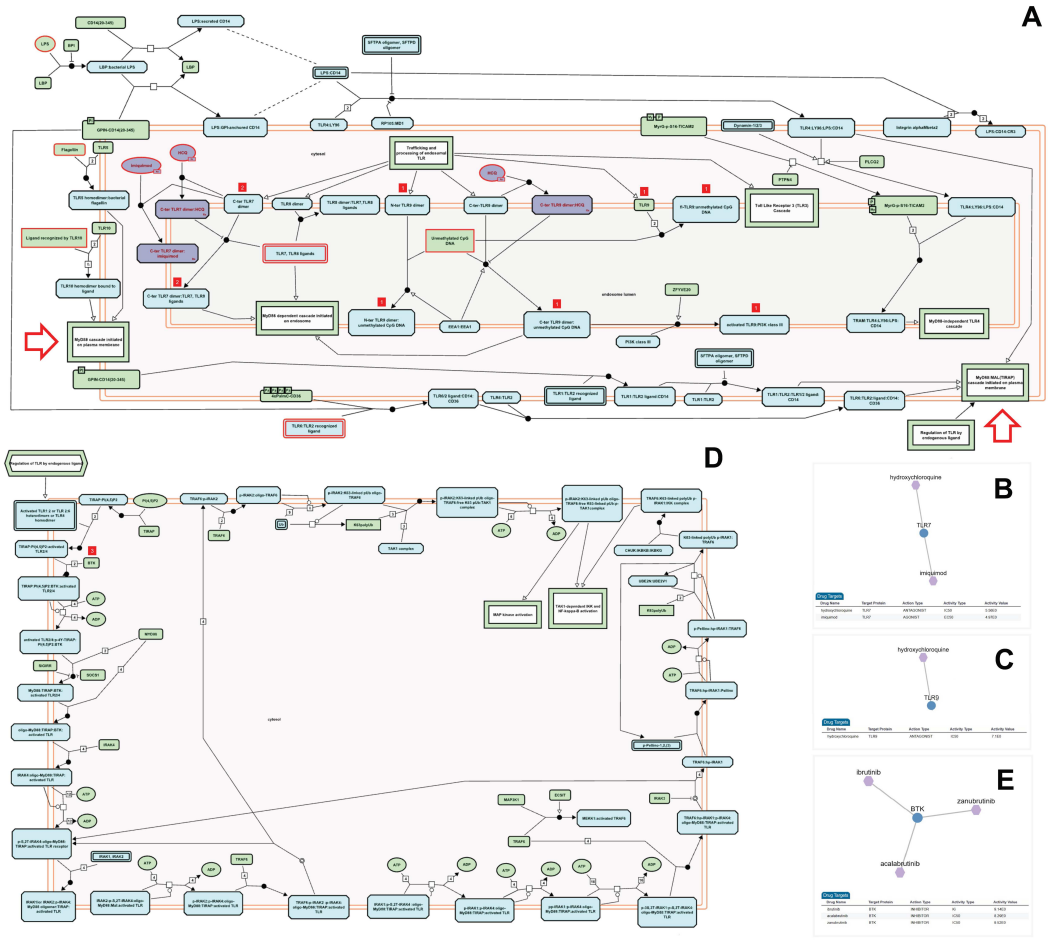

List of local investigators from the participating clinical sites

Jacques-Olivier Pers[1], Alain Saraux[1], Valérie Devauchelle-Pensec[1], Sandrine Jousse-Joulin[1], Bernard Lauwerys[2], Julie Ducreux[2], Anne-Lise Maudoux[2], Ana Tavares[3], Esmeralda Neves[3], Raquel Faria[3], Mariana Brandão[3], Ana Campar[3], António Marinho[3], Fátima Farinha[3], Isabel Almeida[3], Miguel Angel Gonzalez-Gay Mantecón[4], Ricardo Blanco Alonso[4], Alfonso Corrales Martínez[4], Ignasi Rodríguez-Pintó[5], Gerard Espinosa[5], Rik Lories[6], Nicolas Hunzelmann[7], Doreen Belz[7], Niklas Baerlecken[8], Michael Zauner[9], Michaela Lehner[9], Eduardo Collantes[10], M Angeles Aguirre-Zamorano[10], Alejandro Escudero-Contreras[10], Mª Carmen Castro-Villegas[10], Norberto Ortego[11], María Concepción Fernández Roldán[11], Enrique Raya[12], Inmaculada Jiménez Moleón[12], Enrique de Ramon[13], Isabel Díaz Quintero[13], Pier Luigi Meroni[14], Tommaso Schioppo[14], Carolina Artusi[14], Carlo Chizzolini[15], Aleksandra Zuber[15], Donatienne Wynar[15], Attila Balog[16], Magdolna Deák[16], Márta Bocskai[16], Sonja Dulic[16], Gabriella Kádár[16], Falk Hiepe[17], Silvia Thiel[17], Manuel Rodriguez Maresca[18], Antonio López-Berrio[18], Rocío Aguilar-Quesada[18], Héctor Navarro-Linares[18]

Affiliations

1. Centre Hospitalier Universitaire de Brest, Hospital de la Cavale Blanche, Brest, France
2. Pôle de pathologies rhumatismales systémiques et inflammatoires, Institut de Recherche Expérimentale et Clinique, Université catholique de Louvain, Brussels, Belgium
3. Centro Hospitalar do Porto, Portugal
4. Servicio Cantabro de Salud, Hospital Universitario Marqués de Valdecilla, Santander, Spain
5. Department of Autoimmune Diseases, Hospital Clínic, Institut d'Investigacions Biomèdiques August Pi i Sunyer, Barcelona, Catalonia, Spain
6. Katholieke Universiteit Leuven, Belgium
7. Klinikum der Universitaet zu Koeln, Cologne, Germany
8. Medizinische Hochschule Hannover, Germany
9. Medical University Vienna, Vienna, Austria
10. Servicio Andaluz de Salud, Hospital Universitario Reina Sofía Córdoba, Spain
11. Servicio Andaluz de Salud, Complejo hospitalario Universitario de Granada (Hospital Universitario San Cecilio), Spain
12. Servicio Andaluz de Salud, Complejo hospitalario Universitario de Granada (Hospital Virgen de las Nieves), Spain
13. Servicio Andaluz de Salud, Hospital Regional Universitario de Málaga, Spain
14. Università degli studi di Milano, Milan, Italy
15. Hospitaux Universitaires de Genève, Switzerland
16. University of Szeged, Szeged, Hungary
17. Charite, Berlin, Germany
18. Andalusian Public Health System Biobank, Granada, Spain

References

1. https://www.bioinformatics.babraham.ac.uk/projects/fastqc/, last accessed: 2023-03-30.

2. Martin M. Cutadapt removes adapter sequences from high-throughput sequencing reads. EMBnetjournal. 2011 2011-05-02; 17(1):3.

3. Dobin A, Davis CA, Schlesinger F, Drenkow J, Zaleski C, Jha S, et al. STAR: ultrafast universal RNA-seq aligner. Bioinformatics. 2013 Jan 1; 29(1):15-21.

4. Li B, Dewey CN. RSEM: accurate transcript quantification from RNA-Seq data with or without a reference genome. BMC Bioinformatics. 2011 Aug 4; 12:323.

5. Yang X, Regan K, Huang Y, Zhang Q, Li J, Seiwert TY, et al. Single sample expression-anchored mechanisms predict survival in head and neck cancer. PLoS Comput Biol. 2012 Jan; 8(1):e1002350.

6. Perez-Rathke A, Li H, Lussier YA. Interpreting personal transcriptomes: personalized mechanism-scale profiling of RNA-seq data. Pac Symp Biocomput. 2013:159-170.

7. Anders S, Huber W. Differential expression analysis for sequence count data. Genome Biol. 2010; 11(10):R106.

8. Love MI, Huber W, Anders S. Moderated estimation of fold change and dispersion for RNA-seq data with DESeq2. Genome Biol. 2014; 15(12):550.

9. Jassal B, Matthews L, Viteri G, Gong C, Lorente P, Fabregat A, et al. The reactome pathway knowledgebase. Nucleic Acids Res. 2020 Jan 8; 48(D1):D498-D503.

10. https://reactome.org/download/current/Ensembl2Reactome_All_Levels.txt, last accessed: 2023-02-20.

11. Hayes LJ, Berry G. Comparing the part with the whole: should overlap be ignored in public health measures? J Public Health (Oxf). 2006 Sep; 28(3):278-282.

12. Law CW, Chen Y, Shi W, Smyth GK. voom: Precision weights unlock linear model analysis tools for RNA-seq read counts. Genome Biol. 2014 Feb 3; 15(2):R29.

13. Smyth GK. Linear models and empirical bayes methods for assessing differential expression in microarray experiments. Stat Appl Genet Mol Biol. 2004; 3:Article3.

14. Storey JD, Tibshirani R. Statistical significance for genomewide studies. Proc Natl Acad Sci U S A. 2003 Aug 5; 100(16):9440-9445.

15. Li JC. Effect size measures in a two-independent-samples case with nonnormal and nonhomogeneous data. Behav Res Methods. 2016 Dec; 48(4):1560-1574.

16. Rosnow RL. Effect sizes for experimenting psychologists. Can J Exp Psychol. 2003 Sep; 57(3):221-237.

17. Algina J, Keselman HJ, Penfield RD. An alternative to Cohen's standardized mean difference effect size: a robust parameter and confidence interval in the two independent groups case. Psychol Methods. 2005 Sep; 10(3):317-328.

18. Ruscio J, Mullen T. Confidence Intervals for the Probability of Superiority Effect Size Measure and the Area Under a Receiver Operating Characteristic Curve. Multivariate Behav Res. 2012 Mar 30; 47(2):201-223.

19. Brydges CR. Effect Size Guidelines, Sample Size Calculations, and Statistical Power in Gerontology. Innov Aging. 2019 Aug; 3(4):igz036.

20. Cohen J. F Tests of Variance Proportions in Multiple Regression/Correlation Analysis. In: Cohen J, ed. *Statistical Power Analysis for the Behavioral Sciences*: Academic Press; 1977:407-453.

21. https://scikit-learn.org, last accessed: 2023-03-30.

22. https://ww.statmodels.org/, last accessed: 2023-03-30.

23. Ritchie ME, Phipson B, Wu D, Hu Y, Law CW, Shi W, et al. limma powers differential expression analyses for RNA-sequencing and microarray studies. Nucleic Acids Res. 2015 Apr 20; 43(7):e47.

24. https://matplotlib.org/, last accessed: 2024-01-25.